

Modeling and analysis regarding overhead catenary system based on a dynamics method

LUO JIANGUO², LIU HANG^{2,4}, XU JINGDE³

Abstract. Based on the analytic form calculation methods of contact wire lifted displacement, the index of dynamic characteristic of catenary system PoC (Property of Catenary) is proposed. Through simulation calculation and formula deduce, not only the relationships between design parameters of catenary system and the dynamic response of catenary system subjected to a pantograph uplift force are analyzed, but also it is proved that PoC can demonstrate the dynamic characteristic of catenary system. To deeply explore the methods of employing wave theory to analyze the dynamic characteristic of catenary system, wave propagation model of catenary system is proposed, according to which qualitative analysis of the influence of pantograph and droppers is made.

Key words. High Speed Railway, Overhead Catenary System, Pantograph-Catenary System, Dynamics, modeling.

1. Introduction

In order to realize appropriate contact force of the pantograph and sound quality of the current collection, the mathematical simulation models of the catenary system and the pantograph system have been established, which are with the aim of researching their dynamics performance and interaction [1–3]. The literature [4] points out that it is available to simulate required characteristics of the simulation system model of the Pantograph-OCS (Overhead Catenary System) system. The literature [5] indicates that the linear dynamical model of the time-varying stiffness coefficient

¹Acknowledgment - This study was sponsored by the youth fund of Hebei provincial department of education (grant no. QN2017410), the funds for basic research projects in central universities (grant no. 3142015023) and the national natural science foundation of China (grant no. 51374108).

²School of mechanical-electrical engineering, North china institute of science & technology, Langfang, Hebei, P. R. China

³Institute of higher education, North china institute of science & technology, Langfang, Hebei, P. R. China

⁴Corresponding Author, e-mail: luojianguo_083@126.com

of a single-degree-of-freedom belt has been used to simulate the catenary system. On that basis, literature [6] shows that the contact model of the Pantograph-OCS system has been simplified and it is more practical to simplify the Pantograph-OCS system as a beam structure with moving force load and axial stress rather than a cable structure with moving load. Literature [7] an analytical form equation has been established for the beam model with moving force load and axial stress and the solution of the equation had been found out. Literature [8] suggests that the finite element model of OCS has been established, so that the motion differential equation of the pantograph nonlinear model has been figured out. Literature [9] the finite element model of Simple Catenary Equipment OCS and Pantograph/OCS vertical coupled vibration model have been established, the changing situation of OCS dynamic stress has been found out. As a result, to improve the design of the high-speed electric railway, literature [10] suggests that a simulation model is supposed to be established for the Pantograph-OCS system by the mixed method in tension sections. Literature [11] indicates that the flexible contact line has been modeled as the nonlinear continuous beam structure together with absolute coordinate, so that the metamorphosis phenomenon of the contact line has been studied effectively. Literature [12] the simulation model of the catenary system has been established by the finite element computing method and by virtue of Euler-Bernoulli beam theory, so that the static stress and the vibration model of the contact line have been figured out.

2. Analysis regarding overhead catenary system

2.1. The dynamics model for overhead catenary system

The dynamics of the OCS differs from the static property, and the dynamics of interactivity between the OCS and the lifting force of pantograph must be manifested: firstly, the Overhead Contact Line (OCL) must demonstrate the property of vibration caused by the lifting force; moreover, the dropper tension must change along with the mobility of the lifting force.

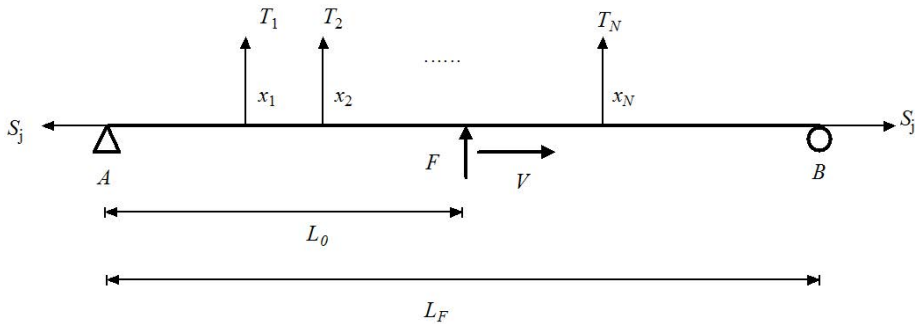


Fig. 1. The model for pantograph coupling system under operation conditions of the single-arm pantograph

The relations between the pantograph and OCL at a certain point of time is shown in Figure 1. The Endpoint A and B represent two terminals of the OCL vibration distortion. In fact, there are no points of support existing at A or B on the OCL, furthermore, vibration distortion does not exist at other parts apart from these two points on OCL. Thus, these two points are assumed as points of support, and the displacement restraint can be realized in the model. T_1, T_2, \dots, T_N are the dropper tension distributed between A and B on the OCL, and x_1, x_2, \dots, x_N represent the positions of the dropper tension that are relative to the pantograph, and N represents the amount of droppers between A and B. F represents the lifting force of the pantograph, that moves along the OCL with a horizontal velocity of V . S_j is the horizontal tension of OCL. L_F represents the OCL length of the vibration tension, L_0 represents the pantograph position between A and B on the OCL that could lead to vibration distortion. Let's assume the movement distance of pantograph with a velocity of V starting from A along the OCL $L_0 = Vt$. According to the wave equation of the catenary model, we can have

$$\begin{aligned}
 m_j \frac{\partial^2 y(x, t)}{\partial t^2} - S_j \frac{\partial^2 y(x, t)}{\partial x^2} &= \frac{F}{l_F} \cdot (u(x - (Vt - \frac{l_F}{2})) - u(x - (Vt + \frac{l_F}{2}))) \\
 &+ \sum_{i=1}^N \frac{T_i}{l_T} \cdot (u(x - (Vt + x_i - \frac{l_T}{2})) \\
 &- u(x - (Vt + x_i + \frac{l_T}{2}))), \tag{1}
 \end{aligned}$$

where m_j is the OCL weight in unit length, l_F and l_T are the distribution lengths of the pantograph lifting force and dropper tension on the OCL respectively, $u(x)$ represents the step function. According to the boundary condition $y(0, t) = y(L_F, t) = 0$, the solution of Equation (1) can be expressed as

$$y(x, t) = \sum_{k=1}^{\infty} W(k, t) \sin \frac{k\pi x}{L_F} \tag{2}$$

and the general solution for the wave equation of the catenary model is

$$y_{\text{hom}}(x, t) = \sum_{k=1}^{\infty} (B_k \sin(\sqrt{\frac{S_j}{m_j} \frac{k\pi t}{L_F}}) + C_k \cos(\sqrt{\frac{S_j}{m_j} \frac{k\pi t}{L_F}})) \sin \frac{k\pi x}{L_F}, \tag{3}$$

where B_k and C_k are undetermined coefficients.

$$C_k = -A_{k2} \sum_{i=1}^N T_i \sin \frac{k\pi x_i}{L_F} \sin \frac{k\pi l_T}{2L_F}, \tag{4}$$

$$B_k = -\frac{V}{\sqrt{S_j/m_j}} (A_{k1} \sin \frac{k\pi l_F}{2L_F} + A_{k2} \sum_{i=1}^N T_i \cos \frac{k\pi x_i}{L_F} \sin \frac{k\pi l_T}{2L_F}). \tag{5}$$

By substituting C_k and B_k to Equation (3), we can have

$$\begin{aligned}
 y(x, t) = & \sum_{k=1}^{\infty} (A_{k1} \sin \frac{k\pi l_F}{2L_F} (\sin \frac{k\pi Vt}{L_F} - \frac{V}{\sqrt{S_j/m_j}} \sin(\sqrt{\frac{S_j}{m_j}} \frac{k\pi t}{L_F})) \\
 & + A_{k2} \sin \frac{k\pi l_T}{2L_F} \sum_{i=1}^N T_i (\sin \frac{k\pi(Vt + x_i)}{L_F} - \frac{V}{\sqrt{S_j/m_j}} \cos \frac{k\pi x_i}{L_F} \sin(\sqrt{\frac{S_j}{m_j}} \frac{k\pi t}{L_F}) \\
 & - \sin \frac{k\pi x_i}{L_F} \cos(\sqrt{\frac{S_j}{m_j}} \frac{k\pi t}{L_F})) \sin \frac{k\pi x}{L_F}, \quad (6)
 \end{aligned}$$

wherein, L_F and T_i can be determined by the calculation result regarding the static uplift of the pantograph lifting force.

2.2. Analysis and calculations regarding the overhead catenary system reflection and dropper phenomenon

It can be illustrated from the OCL vibration displacement Equation (6) that the OCL vibration can be categorized into vibrations caused by the pantograph lifting force and the dropper tension. The OCL vibration displacement Equation (6) directly conduct linear superposition regarding the aforementioned two types of vibrations. The relations among the lifting force of pantograph, changes of the dropper tension, the incident wave, and the reflected wave are demonstrated in Figure 2.

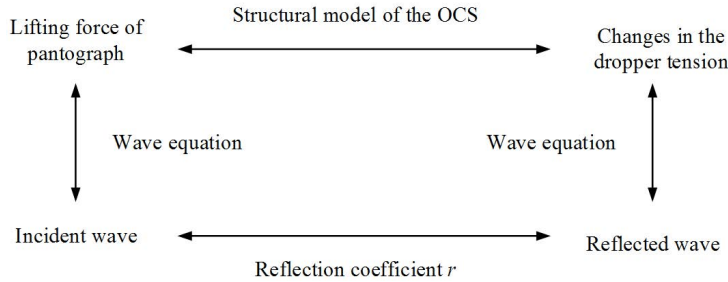


Fig. 2. Relations between the wave and reflection in OCS

Thus, the reflected coefficient is

$$r = \frac{y_r(k, t)}{y_0(k, t)} = \frac{A_{k2} \sum_{i=1}^N T_i \sin \frac{k\pi(Vt + x_i)}{L_F} \sin \frac{k\pi l_T}{2L_F}}{A_{k1} \sin \frac{k\pi Vt}{L_F} \sin \frac{k\pi l_F}{2L_F}}. \quad (7)$$

It can be observed from Equation (7) that the reflected coefficient of OCL is correlated to the dropper tension, therefore the reflected coefficient of OCL differs at different positions, and a variety of design parameters of the OCS have impacts on

the reflected coefficient. If the differences in distribution lengths between the lifting force of pantograph and dropper tension are negligible, namely we assume $l_T = l_F$. Additionally, we replace $\sum_{i=1}^N T_i \sin \frac{k\pi(Vt+x_i)}{L_F}$ by the maximum value of the dropper tension changes $\max[\Delta T]$, then the reflected coefficient can be simplified as

$$r \approx \frac{\max[\Delta T]}{F}. \quad (8)$$

Due to the restriction of droppers to the OCL vibration, the counterforce F_r of the dropper reflective wave will deteriorate the contact conditions of the pantograph: during the process of upward vibration of the OCL, the maximum vibration displacement of the OCL decreases, the contact force of pantograph increases which is $F - F_r$; during the process of downward vibration of the OCL, the minimum vibration displacement of the OCL decreases, the contact force of pantograph decreases which is $F + F_r$. Therefore, according to Equation (1), the OCL motion differential equation is available, after considering the influences from the dropper reflected wave.

$$m_j \frac{tial^2 y(x, t)}{tialt^2} - S_j \frac{tial^2 y(x, t)}{tialx^2} = \frac{F \pm F_r}{l_F} \cdot (u(x - (Vt - \frac{l_F}{2})) - u(x - (Vt + \frac{l_F}{2}))), \quad (9)$$

$$y(x, t) = \sum_{k=1}^{\infty} (A_k \sin \frac{k\pi l_F}{2L_F} (\sin \frac{k\pi Vt}{L_F} - \frac{V}{\sqrt{S_j/m_j}} \sin(\sqrt{\frac{S_j}{m_j} \frac{k\pi t}{L_F}}))) \sin \frac{k\pi x}{L_F}, \quad (10)$$

$$A_k = \frac{4(F \pm F_r)L_F^2/m_j}{(k\pi)^3 l_F (S_j/m_j - V^2)}. \quad (11)$$

Equation (10) demonstrates: changes in the pantograph contact force obtained from reductions of OCS reflection and Doppler Phenomenon can be used to calculate the vibration displacement of the OCS.

3. Simulation regarding the influence of vibration on various design parameters of the OCS

After deriving Equation (10), which is the OCL vibration displacement at the position of pantograph, further analysis regarding the influence of various design parameters of OCS on the OCL vibration displacement is conducted based on previous findings. For convenience of calculation and comparison of results, the paper proposed an index representing the dynamic property of OCS based on Equation (11) regarding the COL vibration, which is called the Property of Catenary (PoC):

$$\text{PoC} = \frac{L_F^2(1 - \max[\Delta T]/F)}{(S_j/m_j - V^2) \cdot m_j}. \quad (12)$$

This index has reflected the value of vibration amplitude of the OCS under the effect of pantograph lifting force F . According to Equation (8), it can be known

that $\max[\Delta T]/F$ is the estimated value of OCS reflection coefficient r . According to the aforementioned assumption, L_F is the OCL length lifted by the pantograph lifting force, which can be more precisely described as the OCL length where residue droppers with tension changes larger than 0.1 N. The simulation will calculate the dynamic property index-PoC at the suspension point and midspan of the Single Catenary System and Stitched Catenary System, and use Equation (10) to calculate the OCL vibration displacement as well as the maximum vibration displacement Y_{\max} , minimum vibration Y_{\min} , the standard deviation of the vibration displacement Y_{std} , and the average vibration displacement Y_m . The pantograph lifting force in all simulative calculations is 116 N, the OCL tension S_j is 25 kN, the unit quality of OCL m_j is 1.1 kg/m, and the pantograph lifting force moves with the velocity of 250 km/h.

3.1. Influence of OCL tension S_j on OCL vibration

When the OCL tension S_j increases, the OCL uplift y_i decreases, the changes of dropper tension ΔT_i reduce, therefore $\max[\Delta T]$ also decreases. Moreover, since $\sum T_i = F$, L_F increases. These two factors will make the PoC increase. However, the increase of the OCL tension S_j will enlarge the fluctuation velocity and decrease the PoC. Therefore, the determination regarding changes in the dynamic property index PoC requires detailed calculations of the OCS design parameters. In general, the outcome associated with the increase of OCL tension S_j will decrease the dynamic property index PoC, as well as the OCL vibration. The simulation results are shown in Table 1.

Table 1. Influences of the OCL tension on OCL vibration

Single Catenary System		OCL Tension S_j			Stitched Catenary System		OCL Tension S_j		
		15 kN	20 kN	25 kN			15 kN	20 kN	25 kN
Midspan	L_F (m)	212.8	212.8	212.8	Midspan	L_F (m)	207.6	207.6	207.6
	$\max[T]/F$	0.2731	0.2286	0.1954		$\max[T]/F$	0.3249	0.2812	0.2472
	PoC (m/N)	3.3953	2.3771	1.8500		PoC (m/N)	3.0009	2.1082	1.6473
Suspension Point	L_F (m)	175.6	200.0	212.8	Suspension Point	L_F (m)	207.6	207.6	207.6
	$\max[T]/F$	0.9772	0.9034	0.8459		$\max[T]/F$	0.8695	0.7852	0.7201
	PoC (m/N)	0.0725	0.2628	0.3544		PoC (m/N)	0.5803	0.6300	0.6125
Y_{\max} (m)		0.0702	0.0524	0.0445	Y_{\max} (m)		0.0759	0.0579	0.0488
Y_{\min} (m)		0.0176	0.0166	0.0149	Y_{\min} (m)		0.0579	0.0456	0.0394
Y_{std} (m)		0.0180	0.0132	0.0105	Y_{std} (m)		0.0045	0.0031	0.0027
Y_m (m)		0.0459	0.0356	0.0308	Y_m (m)		0.0671	0.0525	0.0438

3.2. Influences of the catenary tension S_c on OCL vibration

When the catenary tension S_c increases, the OCL uplift y_i decreases, the dropper tension changes on both sides of the uplift ΔT_i decreases, therefore the $\max[\Delta T]$

increases at the point of lifting forces. Moreover, since $\sum \Delta T_i = F$, L_F decreases. Thus the dynamic property index PoC decreases. The simulation results are shown in Table 2.

Table 2. Influences of the catenary tension S_c on the OCL vibration

Single Catenary System		Catenary Tension S_c			Stitched Catenary System		Catenary Tension S_c		
		15 kN	20 kN	25 kN			15 kN	20 kN	25 kN
Midspan	L_F (m)	212.8	212.8	212.8	Midspan	L_F (m)	207.6	207.6	207.6
	$\max[T]/F$	0.1954	0.2385	0.2731		$\max[T]/F$	0.2065	0.2472	0.2801
	PoC (m/N)	1.850	1.7509	1.6714		PoC (m/N)	1.7363	1.6473	1.5753
Suspension Point	L_F (m)	212.8	200.0	175.6	Suspension Point	L_F (m)	250.0	207.6	207.6
	$\max[T]/F$	0.8459	0.9201	0.9772		$\max[T]/F$	0.6318	0.7201	0.7863
	PoC (m/N)	0.3544	0.1623	0.0357		PoC (m/N)	1.1684	0.6125	0.4676
Y_{\max} (m)		0.0455	0.0386	0.0357	Y_{\max} (m)		0.0579	0.0488	0.0423
Y_{\min} (m)		0.0149	0.0119	0.0089	Y_{\min} (m)		0.0477	0.0394	0.0339
Y_{std} (m)		0.0105	0.0095	0.0087	Y_{std} (m)		0.0034	0.0027	0.0023
Y_m (m)		0.0308	0.0259	0.0225	Y_m (m)		0.0520	0.0438	0.0382

3.3. Influences of the span length L and dropper distribution on OCL vibration

Table 3. Influences of the catenary tension S_c on the OCL vibration

Single Catenary System		Span L			Stitched Catenary System		Span L		
		40 m	50 m	60 m			40 m	50 m	60 m
Midspan	L_F (m)	170.24	212.8	255.36	Midspan	L_F (m)	166.08	207.6	249.12
	$\max[T]/F$	0.1954	0.1954	0.1954		$\max[T]/F$	0.2472	0.2472	0.2472
	PoC (m/N)	1.1840	1.8500	2.6641		PoC (m/N)	1.0543	1.6473	2.3722
Suspension Point	L_F (m)	170.24	212.8	255.36	Suspension Point	L_F (m)	166.08	207.6	249.12
	$\max[T]/F$	0.8459	0.8459	0.8459		$\max[T]/F$	0.7201	0.7201	0.7201
	PoC (m/N)	0.2268	0.3544	0.5103		PoC (m/N)	0.3920	0.6125	0.8820
Y_{\max} (m)		0.0353	0.0445	0.0536	Y_{\max} (m)		0.0389	0.0488	0.0586
Y_{\min} (m)		0.0117	0.0149	0.0181	Y_{\min} (m)		0.0314	0.0394	0.0474
Y_{std} (m)		0.0084	0.0105	0.0125	Y_{std} (m)		0.0022	0.0027	0.0034
Y_m (m)		0.0243	0.0308	0.0368	Y_m (m)		0.0350	0.0438	0.0530

Since changes in the span length will inevitably cause changes in dropper distribution, a more detailed discussion is needed regarding the structural changes. The spaces between droppers expands pro rata, the amount of droppers remains constant, and the span L expands. As the spaces change in a pro rata manner, the force conditions of OCS remain constant, namely the dropper tension change ΔT_i

remains still, therefore $\max[\Delta T]$ remains still. However, due to the increase of the span L , L_F increases accordingly. Thus, the dynamic property index PoC increases, so does the OCL vibration. The simulation results are shown in Table 3.

4. Conclusion

Based on the wave theory, an equation derivation method with an analytical form is adopted to establish the OCS model, and build the nonlinear relations between the travelling wave parameter and the contact force of the pantograph, thereafter qualitatively analyze the influences of the non-uniform qualities and concentrated forces on wave propagation, reflection and transmission. The dynamic property model of the OCS is proposed by combining the catenary structural force model and the mode superposition theory, which can effectively manifest the influences of various design parameters of the OCS on the dynamic property of the OCS.

References

- [1] G. POETSCH, J. EVANS, R. MEISINGER, W. KORTUEM, W. KRABACHER: *Pantograph/catenary dynamics and control*. Vehicle System Dynamics 28 (1988), 159–195.
- [2] W. H. ZHANG, B. HUANG, G. M. MEI: *Study on pantograph-catenary system based on virtual prototyping*. Journal of The China Railway Society 27 (2005), 30–35.
- [3] Y. LIU, W. H. ZHANG, B. HUANG: *Experiment and simulation on dynamic response of the catenary in high-speed railway*. China Railway Science 26 (2005), 106–109.
- [4] A. COLLINA, S. BRUNI: *Numerical simulation of pantograph-overhead equipment interaction*. Vehicle System Dynamics 38 (2002), 261–291.
- [5] T. WU, M. BRENNAN: *Basic analytical study of pantograph-catenary system dynamics*. Vehicle System Dynamics 30 (1998), 443–456.
- [6] T. WU, M. BRENNAN: *Dynamic stiffness of a railway overhead wire system and its effect on pantograph-catenary system dynamics*. Journal of Sound and Vibration 219 (1999), 483–502.
- [7] T. DAHLBERG: *Moving force on an axially loaded beam-with applications to a railway overhead contact wire*. Vehicle System Dynamics 44 (2006), 631–644.
- [8] G. M. MEI, W. H. ZHANG: *Dynamics model and behavior of pantograph/catenary system*. Journal of Traffic and Transportation Engineering 22 (2002), 20–25.
- [9] Y. LIU, W. H. ZHANG, G. M. MEI: *Study of dynamic stress of the catenary in the pantograph/catenary vertical coupling movement*. Journal of The China Railway Society 25 (2003), 23–25.
- [10] G. M. MEI, W. H. ZHANG, H. Y. ZHAO, L. M. ZHANG: *A hybrid method to simulate the interaction of pantograph and catenary on overlap span*. Vehicle System Dynamics 44 (2006), 571–580.
- [11] J.-H. SEO, S.-W. KIM, I.-H. JUNG, T.-W. PARK, J.-Y. MOK, Y.-G. KIM, J.-B. CHAI: *Dynamic analysis of a pantograph-catenary system using absolute nodal coordinates*. Vehicle System Dynamics 44 (2006), 615–630.
- [12] W. H. ZHANG, Y. LIU, G. M. MEI: *Evaluation of the coupled dynamical response of a pantograph-catenary system: contact force and stresses*. Vehicle System Dynamics 44 (2006), 645–658.